ELSEVIER

Biochimica et Biophysica Acta 1371 (1998) 371–381

BIOCHIMICA ET BIOPHYSICA ACTA
BBA

Phototransformation and proton pumping activity of the 14-fluoro bacteriorhodopsin derivatives

Anna B. Druzhko [a,*,1], Baldwin Robertson [a], Rosana Alvarez [b], Angel R. de Lera [b], Howard H. Weetall [a]

[a] *Biotechnology Division, National Institute of Standards and Technology, Gaithersburg, MD 20899, USA*
[b] *Department of Organic Chemistry, University of Santiago de Compostela, Santiago de Compostela, Spain*

Received 6 October 1997; revised 20 January 1998; accepted 13 February 1998

Abstract

The photoinduced behavior and proton pumping characteristics of some bacteriorhodopsin (BR) analogs with fluorinated chromophores (all-*trans* 14-fluorinated [14-F] retinal and 13-*cis* 14-F retinal) derived from wild type (WT) and D96N mutant BR were investigated. These analogs were characterized using spectrophotometry and a highly sensitive electrochemical technique. Similar to the white membrane JW2N, the apomembranes WT ET 1000 and D96N form photoactive pigments with the 14-F chromophores. The resulting analogs have a major absorption band at 588 nm. Red-shifted pigment ($\lambda_{max} \leq 680$ nm) has been previously observed as a minor component of the major 587-nm pigment in 14-F BR made with white membrane JW2N. A similar red-shifted pigment is formed under yellow light ($\lambda > 500$ nm) only in the 14-F analogs derived from WT ET 1000. The measurements of the photoinduced transformation in 14-F WT analogs show that the photocycle of the major pigment occurs simultaneously with the process in the red region and is partially masked by the formation of the red-shifted species. The 14-F D96N samples have a significantly slower and more complicated photoinduced behavior. Electrochemical measurements show that the photoinduced transformation of the red species is not accompanied by proton transport.

Keywords: Bacteriorhodopsin; Retinal analog; Mutant; Photocycle; Red-shifted species

1. Introduction

Bacteriorhodopsin (BR) is the light-energy-transducing trans-membrane protein–chromophore complex in the purple membrane of *Halobacterium salinarium* [1]. Upon photoexcitation, BR goes through a photocycle during which a proton is pumped from the cytoplasmic side to the extracellular side of the membrane [2]. The key element in the light absorption process and the photocycle of BR is the chromophore retinal, which is attached via a protonated Schiff base to the e-amino group of Lys 216 of the polypeptide chain [3]. Interaction of the protein with the chromophore results in a red shift of absorption ('opsin shift') with respect to that of the protonated Schiff base of retinal [4].

* Corresponding author. Institute of Theoretical and Experimental Biophysics, Russian Academy of Sciences, Pushchino, Moscow region, 142292, Russian Federation. Fax: +7-0967-79-0553; E-mail: druzhko@venus.iteb.serpukhov.su

[1] On leave from the Institute of Theoretical and Experimental Biophysics, Russian Academy of Science.

0005-2736/98/$19.00
PII S0005-2736(98)00038-8

A powerful tool for investigating the architecture of the chromophore binding site and chromophore–protein interaction is to replace the natural chromophore with retinal analogs. Recent studies along this line used isotopically labeled retinals [5], a series of dihydroretinals [6] and demethylretinals [7] and 4-keto retinal [8]. These studies have provided significant information on the steric and electronic properties of the chromophore binding site.

Because of its thermal stability and unique photochemical properties, BR is an excellent candidate for use in optoelectronic devices [9,10]. Replacing the chromophore changes the kinetic properties of the native protein–chromophore complex making it more suitable for some applications [11]. This approach can also be used to shift the BR absorption spectrum while maintaining the photochromic activity of the pigment. Of particular interest are chromophore replacements that shift the initial absorbance to the red. This permits using inexpensive semiconductor lasers as a part of the optoelectronic device.

There have been several efforts to prepare unusually red-shifted pigments. One of the reported cyanide-dye pigments produced a BR analog with an absorbance maximum at 662 nm [12]. The other reported red-shifted analogs contain 4-dimethylaminophenil retinoids (615 nm) [13] or ring-fused retinoids (596 nm) [4] as chromophores. Inserting strong electron-withdrawing halogen substituents in the 13- or 14-positions of the chromophore polyene chain (13-CF_3 and 14-F) also leads to a red shift in the absorbance [14–16]. These studies are of particular interest because they report photochemical activity of the resultant pigments. The 14-fluororetinal, when reconstituted with the white membrane of JW2N strain showed the presence of an extra red-shifted minor BR-analog ($\lambda_{max} \leq 680$ nm) in equilibrium with the major 587-nm pigment [15]. This 680-nm pigment with an additional absorption band at 440 nm was enriched when irradiated and rearranged to the 587-nm pigment at room temperature. The chromophore extraction experiments revealed the all-*trans* geometry for the 680-nm pigment. However, the authors did not report in detail the kinetic characteristics of the photocycles of these analogs and did not report any proton pumping activity.

A very detailed study of an O-like photocycle intermediate was carried out using BR derivatives with artificial chromophores, in particular with 14-F retinal [16]. Authors concluded that long lived red-shifted species denoted O_1 can be identified as an unusually long-lived (all-*trans*) intermediate of the photocycle of BR 13-*cis* isomer. All the results with these derivatives based on WT and some mutants—D96A, E204Q, R82Q and D85N—were considered and analyzed from the point of view of the relationships between 13-*cis* and all-*trans*-BR photocycles, and primarily, on the mechanisms of Asp-85 protonation and of proton release by XH in the proton pump of BR. Unfortunately there is no information regarding the peculiarities of formation of red-shifted species and its interaction with purple species in 14-F D96N derivatives in comparison with those in 14-F WT. D96N BR generated by substituting the Asp-96 residue in the native BR molecule with Asn-96 widely used as a very promising BR derivatives [9,17] because the lifetime of the M-state intermediate in this mutant is one to two orders of magnitude longer than that for BR WT [18]. The detailed study of D96N BR in 4-keto-BR gelatin films have been demonstrated the advantage of this BR-derivative as a recording media when compared to films based on the 4-keto WT BR [19]. Therefore the comparative study of fluorinated WT and D96N should be of particular interest and can provide recommendations what BR-derivatives may be preferable.

We present here the results of reconstituting both all-*trans* and 13-*cis* 14-fluororetinals (Fig. 1) with the

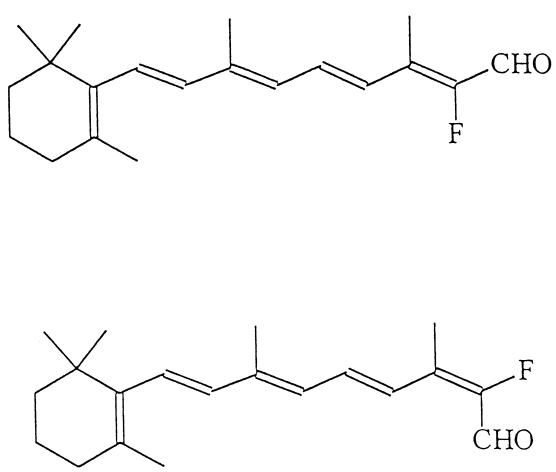

Fig. 1. Chemical structures of fluorinated chromophore analogs used for reconstitution with WT ET 1000 and D96N BR apomembranes.

apomembrane from WT and D96N BR. We describe the photoinduced behavior of the resultant pigments and proton release and uptake.

2. Materials and methods

2.1. Preparation and reconstitution of apomembrane

Suspensions of WT and D96N BR in 0.5 M NH_2OH aqueous solution at pH 8.4 and 7°C were illuminated with visible light ($\lambda > 500$ nm). The activity of the apomembranes was tested by reconstructing with all-*trans* retinal (Sigma, St. Louis, MO). [Commercial names of materials and apparatus are identified only to specify the experimental procedure. They do not imply a recommendation, nor does it imply that they are the best available for the purpose]. The 13-*cis*-14-F retinal and all-*trans*-14-F retinal were prepared as previously reported [20]. Both all-*trans* and 13-*cis* isomers of 14-F retinals, dissolved in iso-propanol (TLC Grade), were used for the reconstruction. The reconstruction procedure was carried out under dim red light at 25°C, pH 6.

2.2. Measurements of photoinduced characteristics

All UV–VIS absorption spectral data and photoinduced absorption changes were measured with a Diode-Array UV/VIS Spectrophotometer (HP 8452A). The maximum power densities of the excitation light (Kodak 300 W Ektagraphic projector) with a yellow long-pass filter ($\lambda > 500$ nm) and an interference filter ($\lambda = 560 \pm 10$ nm) were approximately 30 mW/cm^2 and 3 mW/cm^2, respectively. The pH-dependent photoinduced absorbance changes were measured with the samples diluted in a mixture of 10 mM potassium phosphate, 10 mM TRIZMA base, 10 mM potassium phthalate and 100 mM KCl. All the chemicals were from Sigma.

The light-on and light-off kinetic changes of absorbance were analyzed using one- and two-exponential models. It is well known that in the first portion of the BR photocycle a one-exponential fit for the kinetic processes under the light is quite justified [2]. This function fits the experimental curves with residuals less than 1% of the measured values. For the second portion of the photocycle, when the protein donates a proton to the periplasm and the Schiff base takes a proton from the cytoplasm, [21], more than one exponential is required. The sum of two exponentials fits the light-off kinetics with residuals less than 2% of the measured value. The proton release and subsequent uptake by the 14-F BR-derivatives were measured using an antimony-doped tin-oxide (ATO) coated glass electrode in an electrochemical cell connected to a potentiostat [22].

3. Results

3.1. Reconstitution

The progress of the reconstitution of the all-*trans* and 13-*cis* isomeric forms of 14-F retinal analogs with the apomembranes made from WT BR is shown in Fig. 2. A broad band with a maximum at ≈588

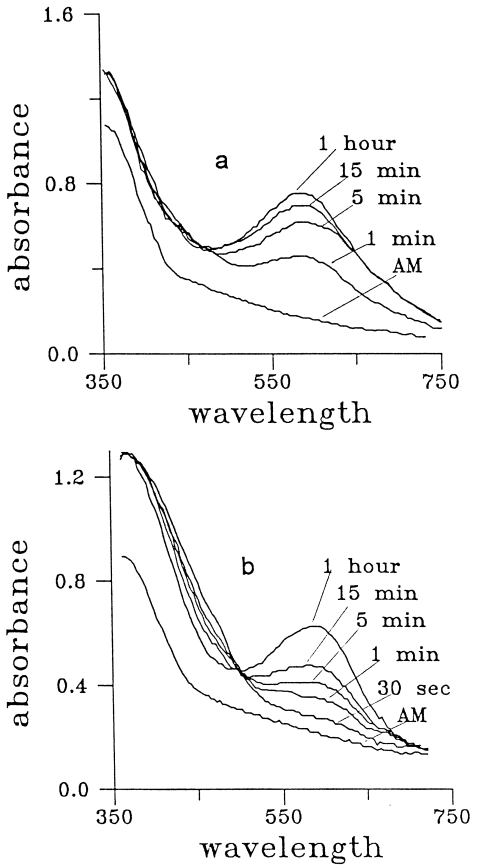

Fig. 2. Absorbance during formation of 14-F BR analogs from (a) all-*trans*-14-F-retinal and (b) 13-*cis* retinal reconstituted with WT ET-1000 apomembranes, pH 6, 25°C, no buffer: The absorbance of both isomers of 14-F D96N formation are similar and so are not shown.

nm appears in all the samples as the reconstitution progresses. Curves for 14-F D96N formation are similar and are not shown. A slight decrease in the 587 nm band and the appearance of an absorption tail in the red region during the reconstitution of the 13-*cis* isomer of 14-F retinal with white membrane JW2N was previously reported [15]. We do not observe a similar formation of red-shifted 680-nm component during reconstitution of 13-*cis* retinal with apomembranes of the WT ET-1000 or D96N pigments (Fig. 2b). A small broad bump is observed in the red region during reconstitution of all-*trans* 14-F retinal with WT apomembranes (Fig. 2a). This bump is mostly expressed in the early stages of reconstitution and almost disappears after it is completed. The reason for different reconstitution spectra of two isomers may be due to the different reconstitution rates for 13-*cis* and all-*trans* 14-F retinals with apomembranes. Most likely there is an equilibrium between the 13-*cis* 14-F and all-*trans* 14-F chromophore isomers after 1 h of reconstruction similar to Tierno et al.'s observation about distribution of isomers of 14-F retinal chromophore during reconstitution with white membranes at the same conditions as we do [15]. Actually it is more appropriate that our resulted pigments would not be further called as 'all-*trans*' and '13-*cis*'.

3.2. Photoinduced spectral transformations

When 560-nm light is turned on at 10°C, red-shifted absorbance bands appear for both the 14-F WT and D96N pigments. The maxima of the differential absorbance are at 640 nm and 650 nm, respectively (Fig. 3). There is a minor absorption band in the 440 nm range for 14-F WT similar to the one reported by Tierno et al. [15] as an additional absorption band for a red-shifted analog. The absorption maximum of the band in the 400 nm range is shifted to the 410–415 nm for 14-F D96N (Fig. 3). The red-shifted species are present at low temperatures in both the 14-F WT and 14-F D96N pigments made from apomembranes and are similar to those present at the same conditions in 14-F WT made from white membranes JW2N [15].

Illuminating the two fluorinated BR analogs with yellow light ($\lambda > 500$ nm) at room temperature leads

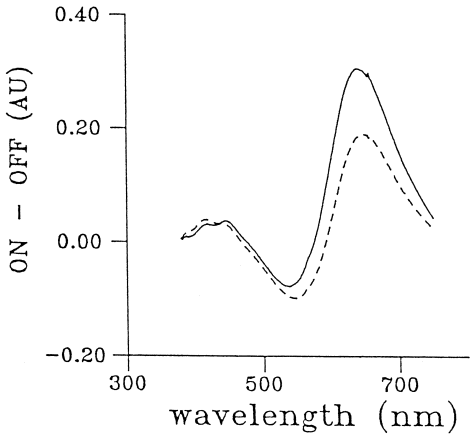

Fig. 3. Differential absorbance spectra (light minus dark) of 14-F WT (solid curve) and 14-F-D96N BR (dashed curve), 560 nm light in 5 min, pH 7, 10°C, no buffer.

to more complicated transformations. The measurements were performed at pH 5, 7 and 9. When the light is turned on, the initial absorbance in the 500 nm range disappears, and an absorption band in the 400 nm range appears for all the samples (Fig. 4a,b). However the light-on absorbance in the 600 nm range appears simultaneously only for 14-F analogs made from WT (Fig. 4a). At pH 5, there is a weak absorbance band in the 400 nm range and a strong absorbance in the 600 nm range. Increasing the pH led to an increase in the optical density and a blue shift of the absorbance in 400 nm range to 420 nm. On the contrary, 14-F analog D96N BR, when illuminated with yellow light ($\lambda > 500$ nm), showed no rise in absorbance in the 600 nm range, but did show a rise in absorbance in the 400 nm range (maximum at ≈ 412 nm) (Fig. 4b). Increasing the pH of the 14-F D96N from 5 to 9 does not cause a blue shift nor the increase in the absorption that is observed for 14-F WT BR. Comparison of the spectra (Fig. 4b) shows that these spectral transformations of the 14-F D96N are almost independent of pH.

3.3. Kinetics of photoinduced processes

The kinetic curves of the photoinduced ($\lambda > 500$ nm) absorbance changes in 14-F WT and D96N suspensions at neutral pH, monitored at 588 nm, 412 nm and 660 nm, are presented in Fig. 5. There is a

striking difference between analogs made from the WT pigment and those made from the D96N pigment. The light-on processes of the absorbance increase at 412 nm and the disappearance at 588 nm are surprisingly slower for the 14-F WT analogs than those for the 14-F D96N (Table 1). Although the light-off decay at 412 nm and recovery at 588 nm of 14-F WT and 14-F D96N are qualitatively similar, they are quantitatively different (Table 1). On the other hand the photoinduced behavior at 660 nm of 14-F WT is qualitatively different from that of 14-F D96N (Fig. 5). The absorbance at 660 nm of 14-F WT rises when the light is turned on (formation of red species) and decays when the light is turned off.

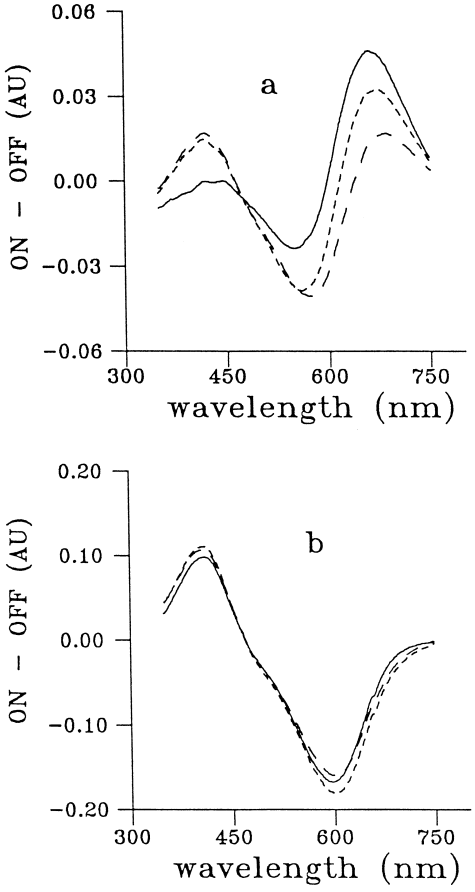

Fig. 4. Differential absorbance spectra (light minus dark) of (a) 14-F WT and (b) 14-F D96N suspended in 100 mM KCl, 10 mM potassium phosphate plus 10 mM Trizma base plus 10 mM potassium phthalate, at pH 5 (solid curve), pH 7 (dashed curve ---) and pH 9 (dashed curve — — —), 20°C. The light is yellow ($\lambda > 500$ nm) and is on for 2 min.

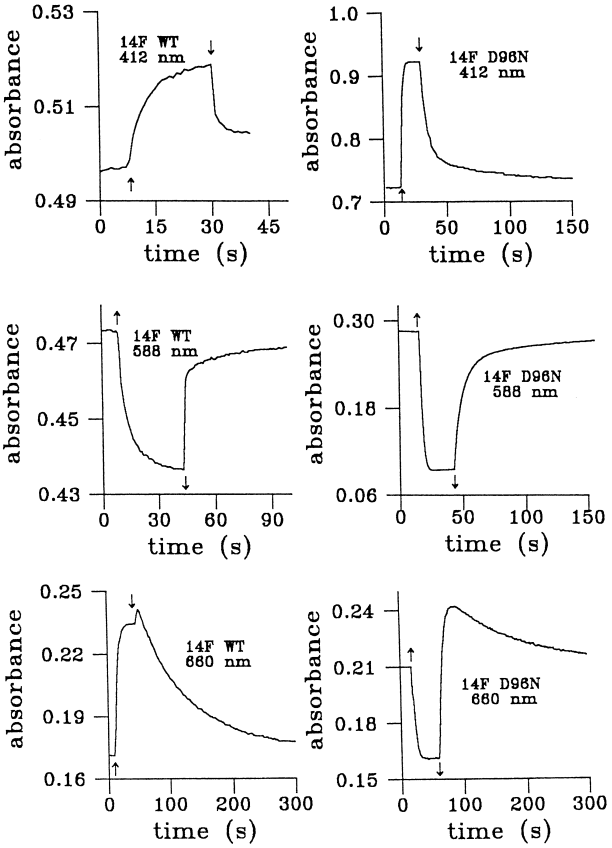

Fig. 5. Photoinduced ($\lambda > 500$ nm) absorbance changes vs. time of 14-F analogs made from WT and D96N monitored at 588 nm, 412 nm and 660 nm, buffer the same as in Fig. 4 at pH 7. ↑ denotes light is turned on, ↓ denotes light is turned off.

In contrast the absorbance at 660 nm of 14-F D96N disappears when the light is turned on, and it first increases and then decays very slowly when the light is turned off.

3.4. pH Dependence of light-on kinetic processes

The time constants of the kinetic curves mentioned above depend on pH (see Figs. 6 and 7). One-exponential curves fit the light-on kinetic processes with residuals $\approx 1\%$. The time constants of the light-on absorbance at 412 nm and 588 nm of 14-F pigments made from WT and D96N decrease slightly with increasing pH (Fig. 6a and b). Similarly the time constants of the light-on changes in the absorbance at 660 nm of 14-F WT decrease with increasing pH

Table 1
Time constants τ_i of the one- or two-exponential fits of the kinetic curves monitored at 412 nm, 588 nm and 660 nm under the yellow light ($\lambda > 500$ nm) and after light exposure

	14-F WT (τ_1, τ_2, ±SD)	14-F D96N (τ_1, τ_2, ±SD)
412 nm light-on	5.99 ± 0.84 s	1.55 ± 0.21 s
588 nm light-on	5.59 ± 0.87 s	1.96 ± 0.28 s
660 nm light-on	4.47 ± 0.61 s up	1.45 ± 0.28 s down
412 nm light-off	0.26 ± 0.02 s; 12.22 ± 2.01 s	4.18 ± 0.66 s; 35.73 ± 5.12 s
588 nm light-off	1.18 ± 0.15 s; 9.18 ± 1.34 s	6.15 ± 0.93 s; 43.75 ± 6.51 s
660 nm light-off	74.27 ± 6.15 s down	5.43 ± 0.71 s up; 102.44 ± 12.3 s down

Buffer the same as for Fig. 3, pH 7, 22°C. The standard deviation (SD) is from three measurements. The notation 'up' and 'down' means the absorbance rises or decreases with time. The light-off slow and fast components for 14-F D96N at 660 nm were fitted by cutting the curve at its maximum and independently fitting a single exponential to the rapid rise and another single exponential to the slow decay.

(Fig. 6c,31). Comparison of Fig. 6a,c,1 shows that the time constants for 14-F WT, monitored at 412 nm and 660 nm, versus pH have similar slopes. The pH-dependence of the time constants of the photoinduced changes at 660 nm for 14-F D96N differs from those for 14-F WT (Fig. 6c,1′) The time constants for the photoinduced absorbance changes at 660 nm in-

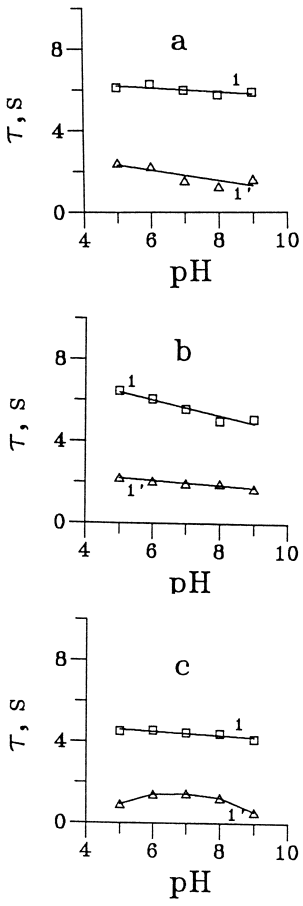

Fig. 6. Time constants vs. pH for the one-exponential fit to the light-on curves of Fig. 5: (**a**) 412 nm, (**b**) 588 nm, (**c**) 660 nm, (1) 14-F-WT, □; (1′) 14-F-D96N, △.

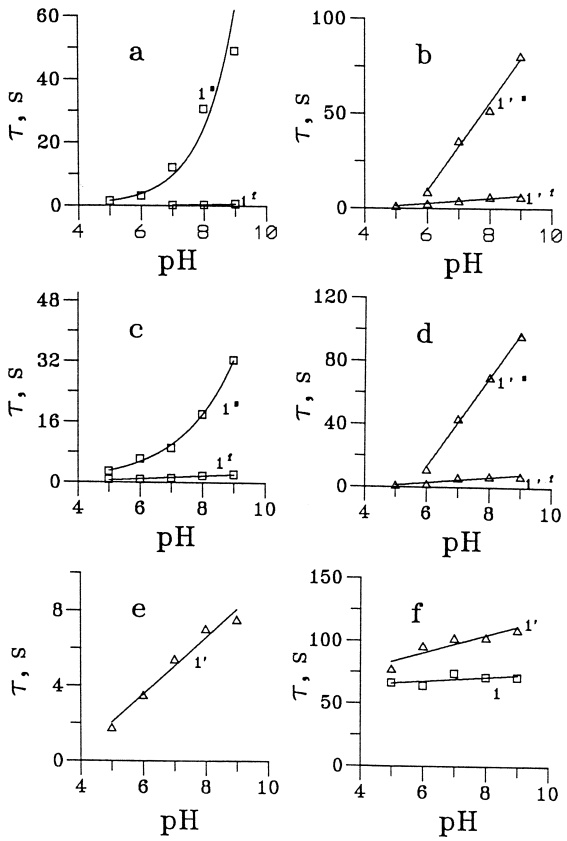

Fig. 7. Time constants vs. pH for the one-exponential (at 660 nm) and two-exponential (at 412 nm and 588 nm) fits to the light-off curves of Fig. 5: 's' and 'f' superscript marks mean slow and fast components, respectively: (**a**) 412 nm, (1) 14-F-WT, □; (**b**) 412 nm, (1′) 14-F-D96N, △; (**c**) 588 nm, (1) 14-F-WT, □; (**d**) 588 nm, (1′) 14-F-D96N, △; (**e**) 660 nm, (1′) 14-F-D96N, △; (**f**) 660 nm, 1-14-F-WT, □; (1′) 14-F-D96N, △.

crease slightly with increasing pH from 5 to 7. The further increase in pH up to nine results in a decrease in the time constants. Although the slopes of the pH-dependence lines at 412 nm and 660 nm are similar for 14-F WT (Fig. 6a,c,1) there is no similarity of pH-dependence character at 412 nm and 660 nm for 14-F D96N (Fig. 6a,c,1′).

3.5. pH-Dependence of the light-off kinetic processes

The pH-dependence of the time constants for the light-off curves (Fig. 7), is much stronger than of those for the light-on curves (Fig. 6). The sum of two exponentials fits the kinetic curves at 412 nm and 588 nm with residuals 1–2% of the measured values. There are two components—fast and slow—for the 412 nm decay and the 588 nm recovery. The fast components of both the 412-decay and the 588-recovery depend very slightly on pH for both pigments (Fig. 7a–d,1^{f},$1'^{f}$). The slow components depend strongly on pH for both WT and D96N. The time constants of the slow components of 14-F WT increase exponentially with pH (Fig. 7a,c,1^{s}), that is they depend much less on pH from 5 to 7 than from 7 to 9.The slow time constants of 14-F D96N increase linearly with pH over the entire pH-range (Fig. 7b,d,$1'^{s}$). The time constants of the 660-nm decay of both pigments depend only very slightly on pH (Fig. 7f).

4. Photocurrent measurements

The photocurrent transients generated by yellow light in 14-F-WT and 14-F-D96N unoriented films on antimony-doped tin-oxide electrodes were measured (Fig. 8). The results of the measurements of these photocurrent transients are summarized in Table 2. As indicated, there are significant difference in amplitudes of these photocurrents in comparison with those produced under the same conditions in WT and D96N pigments with natural chromophore.

For D96N with the natural chromophore, the light-on photocurrent transient (proton release) is always larger than the signal for the WT under identical conditions [24]. This is because the M-state decay rate is slowed and there is a larger accumulation of BR in the M-state. The light-off photocurrent transient (proton uptake) is greatly decreased in size and slowed [23]. This is to be expected since the proton uptake depends on the diffusion of protons to the Schiff base.

For D96N with fluororetinal, on the other hand, the light-on peak is significantly smaller than that for respective WT analogs at neutral pH. The light-on current transient (proton release) of 14-F D96N is several hundreds ms slower than that of the 14-F WT. The light-off current transient of 14-F D96N is a very small step followed by a very slow decay toward the baseline. Proton uptake either does not occur or occurs so slowly that it is not easily observed. These results show that the proton transport of 14-F D96N is significantly slowed or stopped.

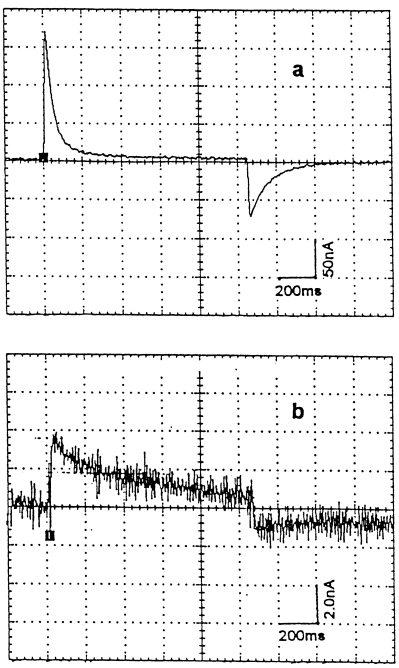

Fig. 8. Photoinduced current transients versus time produced by randomly oriented film of 14-F WT (a) and 14-F D96N (b) analogs of BR on the surface of antimony-doped tin-oxide electrode. The films were illuminated for 1 min with blue light $\lambda < 475$ nm allowed to remain in the dark for 1 min and then illuminated for 1 s with yellow light $\lambda > 500$ nm. All current measurements were performed with 0.05 M potassium chloride with 0.005 M each of potassium citrate, potassium phosphate and potassium borate, pH 7.

Table 2
Measurements of photocurrent peaks at acid and neutral pH

BR-analog samples	pH	Light-on photocurrent peak (±SD)	Light-off photocurrent peak (±SD)
14-F WT	7.0	140 ± 6 nA	−55 ± 3 nA
14-F WT	2.5	−7 ± 1 nA	−[a]
14-F D96N	7.0	4 ± 1 nA	−2 ± 1 nA
14-F D96N	2.5	−2 ± 1 nA	−[a]
WT	7.0	220 ± 8 nA	150 ± 6 nA
D96N	7.0	460 ± 20 nA	20 ± 4 nA

Samples are irradiated with blue light for 1 min before 1 s flash of yellow light. The SDs are for five replicates on the same electrode and represent uncertainty for data collected on a single electrode.
[a]The sample did not show detectable photocurrent.

The time constant of the light-on photocurrent of 14-F WT is less than 100 ms (Fig. 8). The apparatus is not able to measure times shorter than approximately this value. The light-on photocurrent is a measure of proton release in the formation of the M-state. We can say only that the M-state is formed and the proton is released in less than approximately 100 ms.

The comparison of the action spectrum of 14-F WT with the optical absorbance spectrum indicates coincidence in the wavelength of their maxima. It shows that the proton release peaks at 585 nm, not 660 nm (Fig. 9). Attempts to measure the action spectrum of the D96N analogs were unsuccessful since the signal was not sufficiently large to distinguish it from system noise.

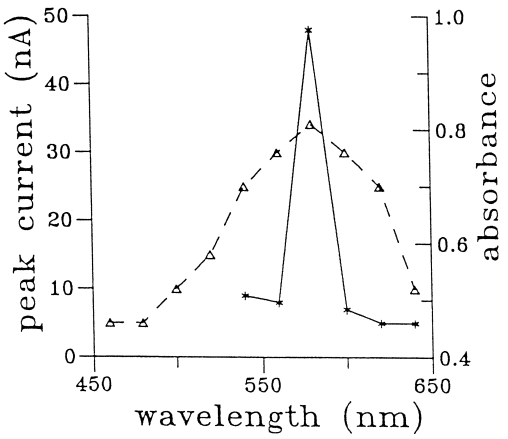

Fig. 9. Action spectra of the light-on peak photocurrents due to the 14-F WT BR compared with the optical absorbance spectra of the respective analog. Electrolyte: 50 mM KCl, 5 mM of each of potassium citrate, potassium phosphate and potassium borate, pH 7.

5. Discussion

5.1. Low- and room temperature spectra

The listed above results indicates the emergence of similar red-shifted bands of absorbance in 14-F WT and D96N under the illumination with 560-nm light at 10°C (Fig. 3) similar to that observed for 14-F BR made from white membrane [15]. The difference between the photoinduced behavior of 14-F WT and that of 14-F D96N at low temperature is small. The additional absorption band at 440-nm, which is characteristic of the red-shifted analog made from white membranes, is observed in 14-F WT and is shifted to 420 nm in 14-F D96N. This shift is due to the contribution of the absorbance at 412 nm of the M-like intermediate, which accumulates because its decay is very slow. At room temperature on the other hand the difference between the photoinduced behavior of 14-F WT and that of D96N is large. The differential spectra (light-on minus light-off) over a pH range 5–9 show that absorbance bands appear at 660 nm for 14-F WT, but not in 14-F D96N, when the 500 nm light is turned on (Fig. 4a,b). For the WT the absorbance band at 660 nm increases as pH is decreased from 9 to 5, and at pH 7 and 9 the absorbance in the 400 nm range is shifted from 440 nm to 420 nm. Similar results were obtained by [16] for 14-F WT.

This may suggest that in 14-F WT, yellow light initiates two simultaneous processes. One process is the photocycle of the pigment with an initial absorbance maximum at 588 nm, whose kinetic characteristics depend on pH, and the other is a photoinduced formation of the red-shifted species at 660 nm. The blue shift and the increase of the absorbance in the 400-nm range are due to the accumulation of the slow M-like intermediate which has an absorbance peak at 412 nm. The blue shift is not seen at pH 5 because the 588-nm photocycle is very fast in comparison with the phototransformation of the red-shifted absorbance. Thus the differential spectra reflect mostly the formation of the red species. In 14-F D96N, light generates the same two processes, but we observe only the first one under the light because the photocycle is much slower, than those for 14-F WT. This statement is confirmed by the results of Gat et al. [16] in a part of 14-F WT about the floating equilibrium between purple and red species, which depend on pH.

5.2. Kinetics

The kinetic curves of the photoinduced absorbance changes at 412 nm, 588 nm, and 660 nm for 14-F WT and D96N (Fig. 5) characterize these two processes in detail. For 14-F WT, when the light is turned on, the 588-nm absorbance disappears, the 412 nm absorbance rises, and the 660-nm absorbance rises (red-shifted species formation). These absorbance changes occur simultaneously. In contrast for 14-F D96N when the light is turned on, the 660-nm absorbance disappears, and when the light is turned off, the 660-nm absorbance reforms and then decays very slowly. That is, the red-shifted absorbance appears as the photocycle of 588-nm state is completing. As mentioned above, there is a thermal equilibrium between isomers after 1 h of reconstitution and we cannot advocate what photocycle these two processes belong to in reference to Gat et al.'s statement [16] that red-shifted species belong to the 13-*cis* photocycle. Our results do not confirm for sure this statement.

5.3. Light-on processes

The 588 nm photocycle for 14-F WT is partially masked by the red-shifted species formation regardless of what photocycle it belong to. First, the time constant of the light-on absorbance increase observed at 412 nm for 14-F WT is surprisingly longer than that for 14-F D96N (Table 1). This high value—around 6 s—cannot be due to the M-like intermediate formation, which is much faster. It is evidently due to the contribution of the 440-nm band of the red species absorbance, which is formed simultaneously with the 588-nm photocycle. Second, the time constants observed at 412 nm agree closely with those at 660 nm (Table 1). Third, the slopes of the time constants vs. pH at 412 nm are approximately the same as those at 660 nm (Fig. 6a,c). Fourth, the time constant of the M-formation and the associated proton release as measured by the photocurrent is less than 100 ms (Fig. 8). The surprisingly large values of the 412 nm time constants, their close numerical agreement with those at 660 nm, and the similarity of their slopes suggest that what is observed at 412 nm in 14-F WT is the tail of the red species formation, not the formation of the M-state. Thus the rate of the light-on process observed at 412 nm is determined by the appearance of the red species at 660 nm with additional absorption band at 440 nm, because it is unusually slow. This slowness was observed by Gat et al. [16]. The absorbance observed at 588 nm is on the other hand due to the ground state, which is highly populated, and therefore is much larger then the tail of the 660 nm absorbance. Hence it goes down and not up like the absorbancies at 660 nm and 412 nm.

The kinetic characteristics for 14-F D96N are different from those for 14-F WT. The values (around 1.5 s) of the time constants of the light-on processes at 412 nm, 588 nm and 660 nm of 14-F D96N are roughly equal (Table 1). However the slopes and even the character of the pH dependence at 412 nm and 588 nm are completely different from those at 660 nm (Fig. 6a–c,1′) in contrast with the approximate equality that occurs for 14-F WT (Fig. 6a–c,1). Now, the photocycle for the D96N mutant with the natural chromophore is slower than for WT especially at neutral and alkaline pH [18], and the same slowing occurs for pigments with fluorinated chromophores based on white membrane JW2N as has been mentioned [15]. The slowing of the photocycle of 14-F D96N causes the pigment to accumulate in the M-state, so the ground state is depleted and the absorbance at 588 nm decreases with time. The light-

on absorbance observed at 660 nm goes down because it is just the tail of the 588 nm absorbance, which goes down. Evidently the light-on absorbance changes observed at room temperature are mostly due to the phototransformation of the 588-nm major pigment. The reason why the red-shifted species is not observed lies in a possible competition between two photoprocesses due to their kinetic characteristics.

5.4. Light-off processes

For 14-F WT the fact that the slow time constants of the light-off processes at 412 nm and 588 nm depend much less on pH in the pH range of 5 to 7 and have a stronger pH dependence in the pH range of 7 to 9 (Fig. 7) may be explained in terms of two processes whose relative contribution to the observed absorbance depends on pH. One process is the 588 nm and 412 nm photocycle, and the other is the decay of the red species, which has an additional absorption band at 440 nm. The decay dominates at acid pH (see Fig. 4a) and thus determines the kinetics and the pH-dependence of all the observed time constants. At pH values between 7 and 9, the photocycle of the 14-F WT with the ground state at 588 nm is slowed down and determines the observed light-off absorbance changes and the pH dependence of the time constants at 588 nm and 412 nm.

For 14-F D96N the light-off processes at 412 nm and 588 nm (412-nm decay and 588 nm recovery) are much slower than those for 14-F WT. These processes are accompanied by a rising absorbance at 660 nm (Fig. 5f) with time constants close in value to those for the fast components of the 412-nm decay and 588-nm recovery (Table 1). The first part of the observed at 660 nm is just tail of the absorbance of the 588 nm state, which is much larger than the absorbance of the M-state. However, the observed rise overshoots and then decays very slowly. The overshoot is due to the 660 nm state. The maximum of the overshoot occurs after 412 nm state has nearly completed its decay. This fact cannot be unambiguously interpreted that 660-nm red-shifted species is a product of the decay of the 412-nm state. It is rather to say that because of very slow photocycle for the purple species of 14-F D96N the floating equilibrium between these two different processes is shifted to photocycle of the purple species with M-like state intermediate formation. We cannot be absolutely positive about what photocycle red species belong to. Gat et al. did not present the date regarding these BR derivatives.

5.5. Proton release and uptake

The coincidence of the maxima of the action spectrum of the peak current and optical absorbance spectrum (Fig. 9) indicates that it is the 588-nm BR analog that releases protons when activated by light, and that the red-shifted 660-nm species is not able to release protons, at least to the fast release. This statement is true for the 14-F WT pigment. For 14-F D96N the photocurrent transient is so small that even the 588-nm purple form cannot do the fast release of the proton.

6. Summary

Thus, the spectroscopic data suggest the existence of two processes initiated in both 14-F WT and D96N by yellow light. For 14-F WT they occur simultaneously with the pH-dependent equilibrium between them. For 14-F D96N the photocycle with ground state at 588 nm is followed by the formation of the red species at 660 nm, which begins only after the light is turned off. The photoinduced processes that result in the formation and decay of the red species do not pump protons, or do so too slowly to be detected by photocurrent measurements.

Acknowledgements

The authors are grateful to Drs. John Kasianovicz, Tonya Herne and Anne Plant for valuable expert assistance and useful discussion.

References

[1] W. Stoeckenius, R. Losier, R. Bogomolni, Biochim. Biophys. Acta 505 (1979) 215–275.
[2] T.G. Ebrey, in: M.B. Jackson (Ed.), Thermodynamics of Membrane Receptors and Channels, CRC Press, Boca Raton, FL, 1992, pp. 353–387.
[3] R.R. Birge, Annu. Rev. Biophys. Bioeng. 10 (1981) 315–354.

[4] J. Lugtenburg, M. Muradin-Szweykovska, C. Heeremans, J.A. Pardoen, J. Am. Chem. Soc. 108 (1986) 3104–3105.
[5] J. Lugtenburg, R.A. Mathies, R.G. Griffin, J. Herzfeld, Trends Biochem. Sci. 13 (1988) 388–391.
[6] F. Derguini, D. Dunn, L. Eisenstein, K. Nakanishi, K. Odashima, V.J. Rao, L. Sastry, J. Termini, Pure Appl. Chem. 58 (1986) 719–724.
[7] A.R. de Lera, B. Iglesias, J. Rodriguez, R. Alvarez, S. Lopez, X. Villanueva, E. Padros, J. Am. Chem. Soc. 117 (1995) 8220–8231.
[8] A. Druzhko, S. Chamorovsky, BioSystems 35 (1995) 133–136.
[9] D. Oesterhelt, C. Bräuchle, N. Hampp, Q. Rev. Biophys. 24 (1991) 425–478.
[10] R.R. Birge, R. Gross, in: R. Petty (Ed.), An Introduction to Molecular Electronics, Oxford Univ. Press, New York, 1995, pp. 315–344.
[11] A. Druzhko, S. Chamorovsky, E. Lukashev, A. Kononenko, N. Vsevolodov, BioSystems 35 (1995) 129–132.
[12] F. Derguini, C.G. Caldwell, M.G. Motto, V. Balogh-Nair, K. Nakanishi, J. Am. Chem. Soc. 105 (1983) 646–648.
[13] M. Sheves, N. Friedman, A. Albeck, M. Ottolenghi, Biochemistry 24 (1985) 1260–1265.
[14] W. Gärtner, D. Oesterhelt, P. Towner, J. Am. Chem. Soc. 103 (1981) 7642–7643.
[15] M.E. Tierno, D. Mead, A.E. Asato, R.S.H. Liu, N. Sekiya, K. Yoshihara, C.-W. Chang, K. Nakanishi, R. Govindjee, T.G. Ebrey, Biochemistry 29 (1990) 5948–5953.
[16] Ya. Gat, N. Friedman, M. Sheves, M. Ottolenghi, Biochemistry 36 (1997) 4135–4148.
[17] N. Hampp, R. Thoma, D. Oesterhelt, C. Bräuchle, Appl. Opt. 31 (1992) 1834–1841.
[18] M. Holz, L.A. Drachev, T. Mogi, H. Otto, A. Kaulen, M. Heyn, V. Skulachev, G. Khorana, Proc. Natl. Acad. Sci. U.S.A. 86 (1989) 2167–2171.
[19] A.B. Druzhko, H.H. Weetall, Thin Solid Films 293 (1–2) (1997) 281–284.
[20] A. Francesch, R. Alvarez, S. Lopes, A. de Lera, J. Org. Chem. 62 (1997) 310–319.
[21] G. Varo, J.K. Lanyi, Biochemistry 29 (1990) 2241–2250.
[22] H. Weetall, A. Druzhko, A. de Lera, R. Alvarez, B. Robertson, Bioelectrochem. Bioenerg. (1998) (in press).
[23] T.V. Dyukova, B. Robertson, H. Weetall, BioSystems 41 (1997) 91–98.
[24] B. Robertson, E.P. Lukashev, Biophys. J. 68 (1995) 1507–1517.